

Supplement of Hydrol. Earth Syst. Sci., 25, 147–167, 2021
<https://doi.org/10.5194/hess-25-147-2021-supplement>
© Author(s) 2021. This work is distributed under
the Creative Commons Attribution 4.0 License.



Supplement of

The role and value of distributed precipitation data in hydrological models

Ralf Loritz et al.

Correspondence to: Ralf Loritz (ralf.loritz@kit.edu)

The copyright of individual parts of the supplement might differ from the CC BY 4.0 License.

Supplement A: Detailed description of the distributed rainfall data

The distributed precipitation data used in this study is based on single-polarization C-band Doppler radar measurements merged with data from rain gauges, micro rain radars and disdrometer observations (Tab. S1). The mainly used radar data is from the radar located in Neuheilenbach, Germany and operated by the German Weather Service (DWD). The raw volume data set has an azimuthal resolution of 1° and a radial resolution of 500 m. The -3dB beamwidth of the antenna is 1° . The radar site is between 40 and 70 km away from the Attert basin. This means that the resolution is yet neither significantly degraded by the beam spreading, nor partial blinded through cone of silence issues. During the period from the 1st of October 2013 to the 27th of March 2014, the radar in Neuheilenbach was out of service due to maintenance issues. We hence used data from a radar located in Wideumont, Belgium in this period. The radar in Wideumont is operated by the Royal Meteorological Institute of Belgium (RMI) and is also a C-band Doppler radar with the same technical specifications as the radar of the DWD. The distance between radar site in Wideumont and the Attert basin is between 24 to 44 km. Thus, the same statements about the resolution, which were made in the case of the data from Neuheilenbach, also apply to the radar data of Wideumont.

15

The data was quality controlled and a correction was performed. The particular raw data was at first filtered by a static clutter filter and then also by a Doppler clutter filter. Subsequently, a bright-band correction (*Hannesen, 1998*) was applied. Occasional contamination of the data by second trip or anaprop echoes was removed by using approaches of *Bückle (2009)* and *Neuper (2009)*. Specific attenuation corrections were not applied. Furthermore, the data was carefully quality checked by an experienced radar meteorologist and operational weather forecaster, who even spends his spare time watching radar pictures. From the corrected data a pseudo PPI (plan position indicator) data set at 1500m above ground was created and afterward an adequate (based on the synoptic situation) reflectivity-rain rate relation (Z-R relation) was applied to compute the precipitation rate (e.g. *Fabry, 2015*). In the last step, the distributed precipitation fields were checked against quality-controlled rain gauges and if necessary manually corrected.

25

Table S1 Location of the distrometer and micro rain radars (*Neuper and Ehret, 2019*)

Station	longitude	latitude	device
---------	-----------	----------	--------

Ell	5.844	49.765	disdro ¹ .
Hostert-Folschette	5.87	49.812	disdro.
Oberpallen	5.847	49.732	disdro.
Petit-Nobressart	5.8	49.779	disdro. / mrr
Post	5.75	49.753	disdro.
Useldange	5.96	49.767	disdro. / mrr

¹disdrometer; ² micro rainfall radar

Supplement B: Influence of different bin widths on the number of occupied precipitation bins

In Fig. S1 we illustrate the influence of different bin widths (0.01, 1 and 3 mm hr⁻¹) for the precipitation data. The number of occupied bins indicates the required number of model elements at a given time step neglecting the effect of the model states on the model resolution. The maximum number of occupied precipitation bins depends on the resolution of the precipitation data and is 42 in this study. Fig. S1 highlights that the absolute number of model elements needed to mimic a distributed model depend strongly on the chosen binning width. The binning width should hence be picked carefully and with a certain physical understanding of the processes and landscape under study or identified within a sensitivity approach to balance accuracy of the adaptive model against model resolution.

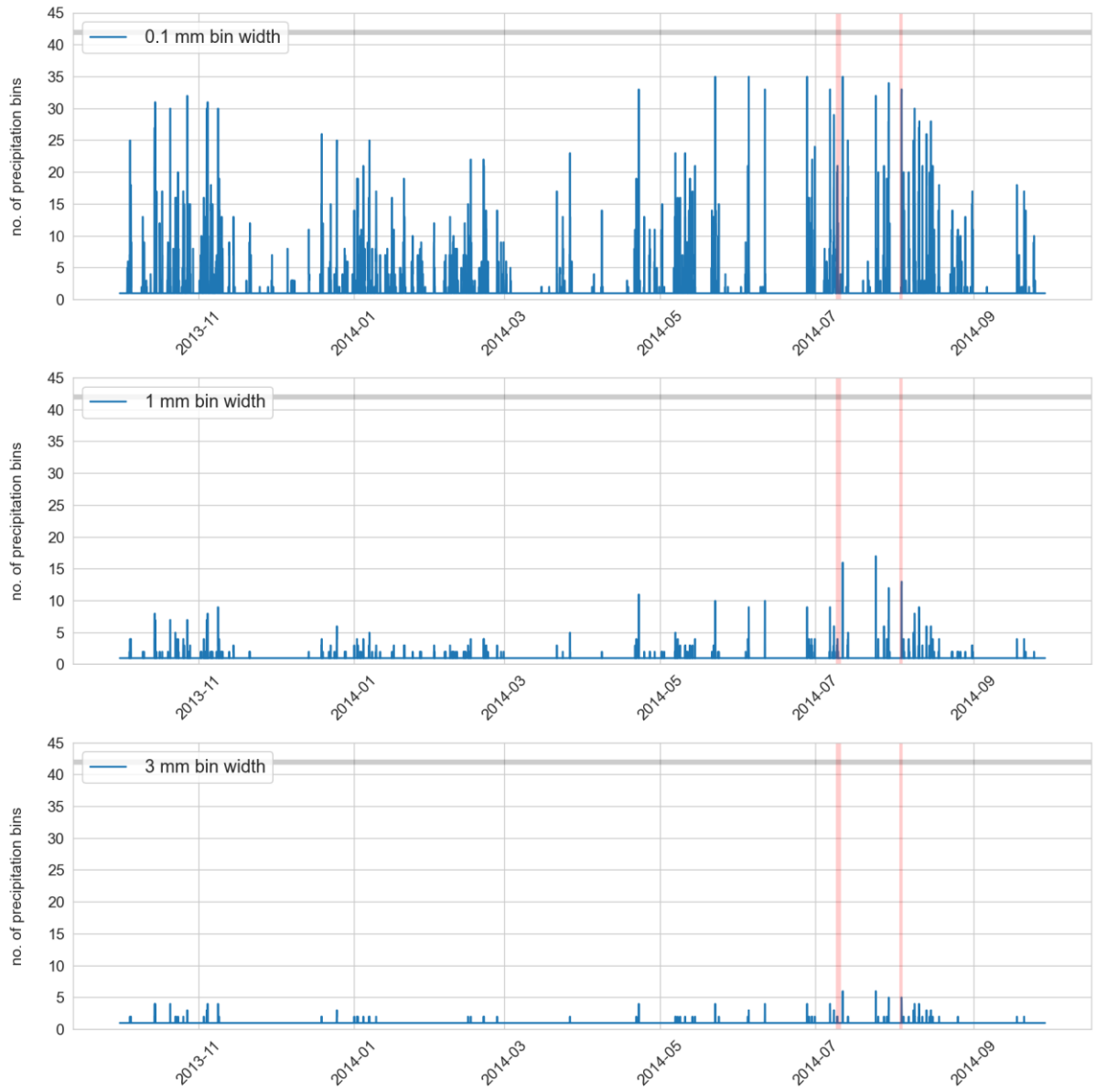


Figure S1 Influence of the bin width on the precipitation data. The horizontal black line displays the maximum number of occupied bins possible to reach given the resolution of the precipitation data of 42 grids. The two vertical red lines show the position of rainfall event I and II.

Supplement C: Model performance measured by the three components of the KGE

Tab. S2 and S3 show the three components of the KGE values displayed in Tab.2 in the manuscript.

Table S2. Model performances (measured by the three components of the KGE) of the reference model, model a and b to simulate the observed discharge of the Colpach catchment based on hourly simulations and observation time steps. The three components are shown for the entire hydrological year (2013/2014) and the summer season.

	annual performance (r = linear correlation)	annual performance (α = flow variability error)	annual performance (β = bias)	summer performance (r = linear correlation)	summer performance (α = flow variability error)	summer performance (β = bias)
reference model	0.9	1.02	0.93	0.72	0.76	0.7
model a	0.91	0.97	0.87	0.8	1.18	0.79
model b	0.93	0.97	0.96	0.84	1.2	1.07

Table S3. Model performances (measured by the three components of the KGE) of the reference model, model a, b and c to simulate the observed discharge of the Colpach catchment based on hourly simulation and observation time steps. The three components are shown for the two selected summer rainfall-runoff events in July and August.

	event I performance (r = linear correlation)	event I performance (α = flow variability error)	event I performance (β = bias)	event II performance (r = linear correlation)	event II performance (α = flow variability error)	event II performance (β = bias)
reference model	0.6	0.58	0.31	0.85	0.15	0.15
model a	0.01	0.8	0.42	0.62	0.34	0.26
model b	0.72	0.48	0.59	0.86	0.32	0.42
model c	0.71	0.48	0.59	0.86	0.31	0.43

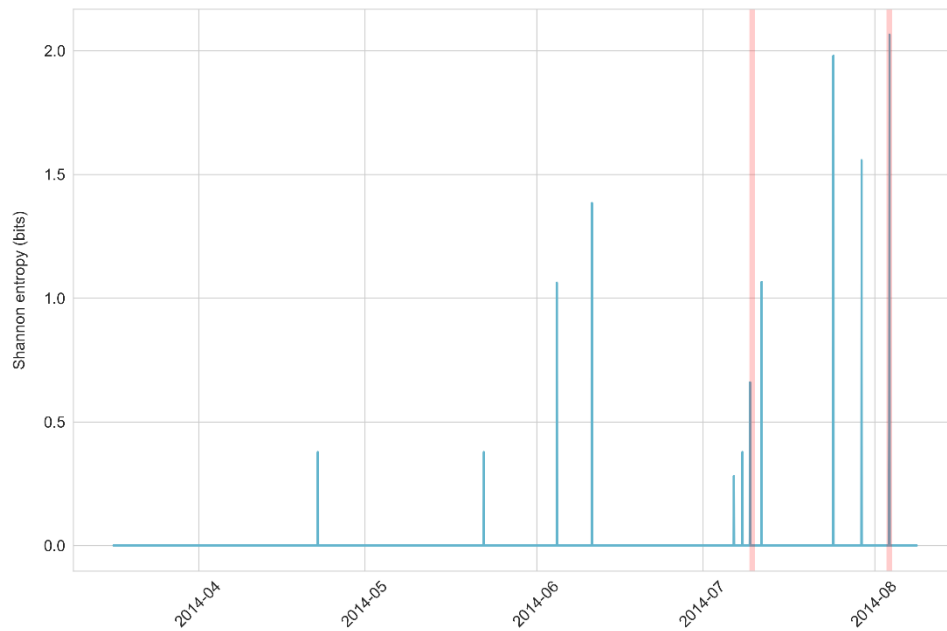
10

Supplement D: Shannon entropy of the distributed model b

In Fig. S2 displays the Shannon entropy of the distributed *model b* for each hourly simulation time step with the same binning used to group / bin the model states of 0.05 mm hr^{-1} for the summer season. The Shannon entropy is introduced in detail in *Cover and Thomas (2005)*. While the Shannon entropy has several interesting features the important part for this study is that a Shannon entropy of zero means that we can compress our distributed

15

model b to a single hillslope (Loritz *et al.*, 2018). The latter means that shortly after the two picked rainfall runoff event does *model b* dissipate the past forcing and all 42 hillslopes simulate the similar hydrographs.



5 **Figure S2 Shannon entropy of the hourly simulation time steps of the distributed model b for the summer season. Red vertical lines indicate the position of the two selected rainfall events.**